

Lead Sorption onto Ferrihydrite. 3. Multistage Contacting

JAMES A. DYER,^{*,†,‡} PARAS TRIVEDI,[†]
STEPHEN J. SANDERS,[§]
NOEL C. SCRIVNER,[‡] AND
DONALD L. SPARKS[†]

Department of Plant and Soil Sciences,
University of Delaware, Newark, Delaware 19717,
DuPont Engineering Technology, Brandywine Building,
Wilmington, Delaware 19898, and OLI Systems, Inc.,
108 American Road, Morris Plains, New Jersey 07950

Few studies have demonstrated the practical application of surface complexation models, calibrated with fundamental macroscopic and spectroscopic metal sorption data, in helping to solve industrial trace metal emissions problems. In this work, multistage ferrihydrite sorption systems are evaluated for their effectiveness in reducing single-solute lead-(II) [Pb(II)] concentrations in contaminated water streams to very low levels. Experimental data and modeling results indicate that a multistage sorption system can significantly reduce Pb(II) effluent concentrations for the same total amount of sorbent or, alternatively, dramatically lower total sorbent consumption for the same effluent Pb(II) concentration. Model predictions were generated using a steady-state, multistage, equilibrium adsorber model that was specifically developed for and integrated into OLI Systems' Environmental Simulation Program. The modified triple-layer model was used to simulate Pb(II) surface–liquid equilibria within the adsorber model. Engineering screening evaluations indicate that a 2–3-stage sorption process can provide significant economic savings when compared to a 1-stage process operating with the same target effluent Pb(II) concentration. Additional equilibrium stages beyond 2 or 3 provide diminishing economic returns. The major economic driver for multiple contacting stages is reduced capital investment and operating costs for sludge handling, dewatering, and disposal.

Introduction

Trace metal discharges from industrial manufacturing processes are being increasingly scrutinized and regulated as new, revised, and proposed regulations are pushing metal effluent limits to parts per billion (ppb) and lower levels (1–5). Alkaline precipitation has historically been the technology of choice for meeting parts per million regulatory levels for trace metals [e.g., Pb(II), Ni(II), Cd(II), Zn(II), etc.] in direct-discharge wastewater point sources; however, this technology is limited to ≥ 1 ppm effluent concentrations because of the finite solubility of amorphous metal hydroxide phases [i.e., PbO, Ni(OH)₂, Cd(OH)₂, Zn(OH)₂, etc.] and

inefficiencies in commercial solid–liquid separation devices (6). On the other hand, much lower effluent levels are possible by taking advantage of the large sorptive capacity of amorphous, high-surface-area solids, such as hydrous iron and aluminum oxides.

Merrill et al. (7) examined the technical and economic feasibility of removing inorganic trace elements, such as arsenic (As) and selenium (Se), from coal-fired power plant wastewater streams via coprecipitation with hydrous ferric oxide (HFO) in a single contacting stage. Removal efficiencies of 80–99% were achieved for 5–140 ppb As(III), As(V), and Se(IV) feed concentrations at pH 7.5–8.5; however, Se(VI) removal was only 5–15%. Testing results showed that optimum metals removal occurred at pH <9 for As(V), pH 8–9 for As(III), pH <7 for Se(IV), and pH <4 for Se(VI). On the other hand, a two-stage cross-flow process (i.e., separate fresh-HFO feeds to each stage) might allow for satisfactory removal of all four contaminants if the two stages are controlled at different pH values (e.g., pH 4.5 and 8.5).

Schultz et al. (8) examined the feasibility of a closed-loop, one-stage process that consisted of metal sorption onto ferrihydrite from dilute solutions at pH 9, followed by desorption into a more concentrated regenerant solution at pH 4.5. Reaction times were 1–3 h in each step. Except for cadmium, a measurable fraction of the bound metals was not easily desorbed. This slowly reversible fraction increased with increasing pH and duration of the high-pH sorption stage and increased more or less continuously in subsequent cycles. Interestingly, the metals retained in the ferrihydrite structure did not affect metals removal in five subsequent cycles for the concentration range studied. Edwards and Benjamin (9) extended the work of Schultz et al. (8) by considering the performance of the regenerated ferrihydrite sorbent over 50 cycles rather than just six. Removal efficiency remained >98% when treating both synthetic and real plating wastes containing 1–3 ppm each of six metals. Adsorption and desorption cycle times were reduced from 1–3 h to 10 and 10–30 min, respectively. Preformed ferrihydrite solids (0.45 g/L) were found to aid removal of 90% of the suspended sorbent solids within 3 min; only 4% remained suspended after 50 min.

An alternative to batch or continuous stirred-tank reactor configurations for the ex situ treatment of metal-contaminated waters is a fixed-bed column containing a granular sorbent that can be regenerated over many cycles (10–14). Advocates of this alternative approach argue that dynamic flow in fixed beds is preferred over a continuous stirred-tank configuration because it eliminates the need for potentially expensive solid–liquid separation facilities. For example, Smith and Amini (14) investigated removal of 10 ppm lead-(II) [Pb(II)] from a wastewater stream at pH 5.5 in fixed-bed columns containing a recycled, granular, iron-bearing material recovered from surface finishing operations in cast-iron manufacture. While treatment was effective initially, efforts to regenerate the sorbent with aqueous EDTA- and DTPA-chloride salt solutions resulted in relatively low Pb(II) recovery (40–50%) and a subsequent loss of adsorption efficiency. Interestingly, Smith (13) and Smith and Amini (14) used the modified triple-layer model (TLM) to predict metal sorption equilibria onto the recycled iron-bearing sorbents; the iron sorbent was treated as a hydrous ferric oxide in aqueous solution. The modified TLM was integrated into a dual-resistance mass-transport model to simulate the performance of the fixed-bed columns.

There is essentially no discussion in the peer-reviewed literature of using a high-surface-area sorbent, such as HFO

* Corresponding author e-mail: james.a.dyer@usa.dupont.com; phone: (302)774-2237; fax: (302)774-1347.

† University of Delaware.

‡ DuPont Engineering Technology.

§ OLI Systems, Inc.

TABLE 1. Definition of and Results for Pb(II)/Ferrihydrite (fh) Multistage Sorption Case Studies^a

case	stage	g of fh/L in each stage	stage 1 Pb(II) feed concn (ppm)	Pb(II) effluent measd ^b	95% CI Pb(II) effluent measd ^c	Pb(II) effluent model	95% CI Pb(II) effluent model ^c
1A	1	1.0	103.6	2.1 ppm	2.04–2.15 ppm	1.8 ppm	0.97–3.3 ppm
1B	1	0.5	103.6	10.0 ppm	9.3–10.7 ppm	4.5 ppm	2.5–8.5 ppm
	2	0.5		128 ppb	122–132 ppb	57 ppb	12.3–148.6 ppb
2A	1	4.65	10.36	13.7 ppb	10.9–15.5 ppb	10 ppb	5.9–19.8 ppb
2B	1	0.253	10.36	323 ppb	310–340 ppb	462 ppb	272–827 ppb
	2	0.253		5.3 ppb	4.3–6.3 ppb	8 ppb	1.9–20.7 ppb
2C ^d	1	0.08	10.36	na ^e	na	1.8 ppm	na
	2	0.08		na	na	183 ppb	na
	3	0.08		na	na	10 ppb	na
3A	1	0.4	103.6	11.6 ppm	11.1–12.1 ppm	6.2 ppm	3.4–11.5 ppm
3B	1	0.2	103.6	22.0 ppm	21.8–22.6 ppm	17.8 ppm	10.8–31.2 ppm
	2	0.2		1.6 ppm	1.6–1.64 ppm	1.3 ppm	0.39–3.1 ppm
3C	1	0.1	103.6	41.0 ppm	40.6–41.3 ppm	44.3 ppm	34.9–59.1 ppm
	2	0.1		8.2 ppm	8.0–8.3 ppm	10.9 ppm	5.7–20.1 ppm
	3	0.1		0.395 ppm	0.39–0.4 ppm	1.6 ppm	0.35–3.8 ppm
	4	0.1		6.1 ppb	5.8–6.3 ppb	115 ppb	8.1–378 ppb

^a All experiments were conducted at room temperature in a N₂ glovebox using a 0.01 M NaNO₃ background electrolyte solution. The pH in each stage was controlled at 5.5 using 0.1 M HNO₃ or NaOH. ^b Mean of triplicate studies. ^c See ref 37 for more details on how the 95% confidence intervals (CI) were generated. CI for the measured values reflect “same-batch” variation displayed by the triplicate studies. CI for the model values reflect “between-batch” uncertainties in input parameters [i.e., pH, Pb(II), ferrihydrite, and NaNO₃ feed concentrations, and mass H₂O] as well as uncertainties in the thermodynamic parameters (i.e., surface complexation *K* values). ^d ESP simulation only for inclusion in engineering evaluations. ^e na, not applicable.

or ferrihydrite, to treat metals-contaminated wastewater streams to ppb levels in a multistage cross-flow or counter-current-flow reaction system. However, treatment with any high-surface-area sorbent in two or more equilibrium contacting stages will (i) reduce metal effluent concentrations to much lower levels than can be achieved in one stage using an equivalent amount of sorbent or (ii) reduce total sorbent consumption and disposal for the same target effluent concentration. In addition, staging can be used in a cross-flow configuration to optimize the removal of several trace metals and metalloids whose pH ranges for optimum treatment are much different. Experience in the chemical engineering field has shown that 2–4 contacting stages often provide significant improvement over a single contacting stage in chemical reaction, leaching, and extraction systems, while additional stages beyond 4 or so often lead to diminishing economic returns (15–17). A decision on the number of contacting stages often becomes an economic tradeoff between the incremental capital investment for the additional equipment and the savings in raw material, energy, and waste disposal costs.

In this paper, one-, two-, three-, and four-stage ferrihydrite sorption systems are evaluated for their effectiveness in reducing single-solute Pb(II) concentrations to very low levels in contaminated water streams. The objectives of the research were 3-fold. First, to demonstrate how a multistage sorption process can significantly reduce trace metal effluent concentrations for the same total amount of sorbent or, alternatively, dramatically lower total sorbent consumption for the same metal effluent concentration. Second, to develop and validate a steady-state, multistage, adsorber model for treating a Pb(II)-contaminated water stream to parts per billion levels, and in the process, demonstrate the integration of a surface complexation model (SCM), such as the modified TLM, into a steady-state equilibrium process flowsheet simulator to predict metals removal efficiency and sorbent requirements. Third, to conduct engineering screening evaluations to highlight the economic drivers for equilibrium staging.

Methods

Ferrihydrite Preparation. The 2-line ferrihydrite was synthesized, washed, and aged for 48 h according to the procedures described in ref 18.

Multistage Pb(II) Sorption Experiments. Sorption studies were conducted with preformed ferrihydrite solids at room temperature in a N₂ glovebox using 1-L, well-mixed reaction vessels containing a 0.01 M NaNO₃ background electrolyte solution. All studies were conducted in triplicate at the same time using the same batch of ferrihydrite. Equilibration time was 4 h for each contacting stage, and pH was controlled at 5.5 using 0.1 M HNO₃ or NaOH. Lead was added as Pb(NO₃)₂ using a 1 M stock solution. All chemicals were ACS reagent-grade; ultrapure water (Micropore SA) was used throughout. Equilibrated ferrihydrite solids were separated from the aqueous phase using a RC5 Sorvall centrifuge operating at 12 000 rpm for 20 min. Graphite furnace–atomic absorption spectroscopy (Perkin-Elmer Analyst 800) was used to analyze the centrates for total soluble Pb(II). The multistage, cross-flow sorption experiments were batch equilibration studies; the experimental conditions for each case are summarized in Table 1. For example, in a two-stage system, such as case 1B, 0.5 g of “fresh” ferrihydrite sorbent was first equilibrated with 0.5 mmol of Pb(NO₃)₂ dissolved in 1 L of a 0.01 M NaNO₃ background solution (103.6 ppm Pb). After 4 h, the mixture was centrifuged, and the resulting centrate was analyzed for residual Pb(II) in solution. The bulk of the remaining centrate (~0.9 L) was then added to a second 1-L reaction vessel where it was equilibrated again for 4 h with 0.5 g/L fresh ferrihydrite sorbent. The resulting centrate was analyzed for residual Pb(II). More background on the experimental protocol used in this study can be found in ref 18.

Geochemical Modeling Software. The OLI Software (OLI Systems, Inc., Morris Plains, NJ) was used to perform the multistage, steady-state simulations. Details on the thermodynamic databank and framework, the equation solvers, and the SCMs used in the OLI Software are presented in ref 19. More specifically, the Environmental Simulation Program (ESP) was used for this study because it is designed for steady-state simulation of vapor, liquid, and solid interphase and intraphase equilibria occurring within multistage chemical process flow sheets. The modified TLM [as developed by Davis et al. (20) and Davis and Leckie (21), later modified by Hayes and Leckie (22, 23), and finally extended by Sverjensky and Sahai (24)] was utilized in this work because it provided the best fits of the Pb(II)/ferrihydrite isotherm and pH edge data presented and analyzed in refs 18 and 19. The experimental data and TLM

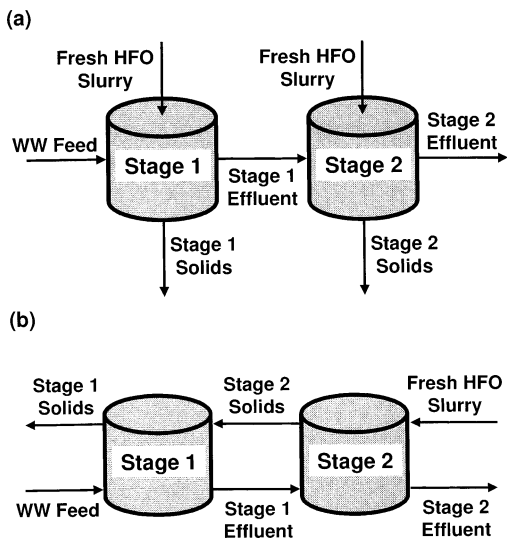


FIGURE 1. Schematic flow diagrams for two-stage cross-flow (a) and countercurrent-flow (b) sorption systems.

calibrations presented in this previous work cover the pH range 3.0–6.5.

Surface Complexation Models. Over the years, a variety of SCMs have been developed and utilized for predicting trace metal sorption onto mineral oxides. These include the nonelectrostatic model (NEM), the constant capacitance model (CCM), the diffuse-layer model (DLM), the generalized two-layer model (GTLM), and the modified triple-layer model (TLM). SCMs attempt to explicitly account for the reaction processes occurring at the solid–water interface; they assume that metal ions form complexes with surface functional groups in a manner similar to metal–ligand complexation reactions in solution (25). They are thermodynamic models that differ in their physical description of the solid–water interfacial region (i.e., the location of sorbed species with respect to the surface as well as the description of surface charge–potential relationships across the interfacial region) and in their assumptions regarding number of site types and the structure and composition of the sorbed species. More background on SCMs can be found in ref 25.

Modeling Protocol. Examples of two-stage cross-flow and two-stage countercurrent-flow sorption systems for treating a metals-contaminated wastewater stream are shown schematically in Figure 1, panels a and b, respectively. In a cross-flow system, fresh sorbent is added to each reaction vessel or stage, equilibrated with the contaminated wastewater, and then removed for dewatering and disposal. This contrasts with a true countercurrent-flow system (Figure 1b) where fresh sorbent is added to the final sorption stage and partially spent sorbent is subsequently reused in the upstream stages (i.e., the flow of sorbent is countercurrent to the flow of wastewater). A true countercurrent-flow system represents the minimum-sorbent-consumption case for a specified metals effluent concentration. For solids handling reasons, a cross-flow arrangement will probably be more practical for amorphous materials, such as ferrihydrite, in most industrial situations. In addition, to simplify the process, most full-scale industrial systems would likely be operated in a coprecipitation mode rather than a sorption (onto preformed floc) mode as shown in Figure 1. The experimental and modeling studies in this work are based on Pb(II) sorption onto preformed ferrihydrite in order to utilize the TLM results from ref 19. Operation in a coprecipitation mode would likely lead to lower Pb(II) effluent concentrations and sorbent requirements; however, the benefits of staging will be realized in either mode. As a result, model predictions based on a

TABLE 2. Triple-Layer Model Parameters Used in ESP Simulations of Multistage Pb(II) Sorption onto 2-Line Ferrihydrite^a

parameter	value
Pb(II) surface species	($\equiv\text{FeO}$) ₂ Pb and $\equiv\text{FeOHPb}^{2+}$
N_s (mol/mol)	0.8
A_s (m ² /g)	600
C_1 (faraday/m ²)	0.725
C_2 (faraday/m ²)	0.2
$\log K_{a1}^{\text{int}}$	-5.41
$\log K_{a2}^{\text{int}}$	-10.41
$\log K_{\text{NO}_3^-}^{\text{int}}$	-7.59
$\log K_{\text{Na}^+}^{\text{int}}$	8.14
$\log K_{(\equiv\text{FeO})_2\text{Pb}}^{\text{int}}$ at 1 g of solids/L ^b	4.98 (pH 4.5–5.5)
	6.16 (pH 6.5)
$\log K_{\text{FeOHPb}^{2+}}^{\text{int}}$	-8.76 (pH 4.5–5.5)
	-5.27 (pH 6.5)
γ_s	$\gamma_s = \gamma_{\text{Pb}^{2+}}$

^a Refer to Tables 1 and 2 in ref 19 for details on the chemical reactions and mass law expressions corresponding to each of the equilibrium constants given above. Definitions for each of the parameters can be found in the nomenclature section of ref 19. Parameters are valid over the pH range of 4.5–6.5, except as noted. ^b For bidentate surface complexes, K^{int} is really a conditional K that depends on sorbent solids concentration. The value for K in this table is based on 1 g of ferrihydrite/L. See Table 2 in ref 19 for additional explanation.

sorption process will be conservative for environmental compliance purposes.

Steady-state process flow sheets were constructed in ESP using the appropriate combination of unit operations (separator, pH controller, acid/base manipulator, and sensitivity blocks) and feed/effluent streams (wastewater feed, sorbent feed, NaOH feed, stage 1 effluent, stage 1 solids, etc.). Separator blocks served as the isothermal reaction vessels. The efficiency of the solid–liquid separation was also specified in this block. An acid/base manipulator block and a pH controller were linked to each separator block to regulate the flow of mineral acid or base to each reaction vessel, so as to control pH at 5.5. The sensitivity block was used to perform multiple-case runs. The TLM functioned within all blocks containing sorbing solids. An example of a block flow diagram for a two-stage ESP cross-flow sorption model is shown in Figure S1 in the Supporting Information.

TLM parameters and associated Pb(II) surface speciation assumptions used in this work were obtained from ref 19 and are summarized in Table 2. These assumptions and parameters are valid over the pH range of 4.5–6.5 as noted in the table. ESP simulations were made for each of the cases listed in Table 1. The objective was to compare model predictions based on the single-solute Pb(II) sorption data reported in ref 18 to the results of the bench-scale multistage experiments. In theory, the results should not be statistically different when taking into account experimental and model uncertainties. In addition, generalized sensitivity studies were conducted over the pH range of 4.5–6.5 to understand the impact of pH, Pb(II) feed concentration, number of stages, perfect versus imperfect solid–liquid separations, and cross-flow versus countercurrent-flow arrangement on the predicted Pb(II) effluent concentration at a fixed sorbent dose and the predicted sorbent requirement at a specified Pb(II) effluent concentration.

Engineering Evaluations. High-spot engineering evaluations ($\pm 30\%$) were completed for each of the cases in Table 1 to assess the relative economic incentive/penalty for additional equilibrium sorption stages. The volumetric flow rate of contaminated wastewater was assumed to be 6.3 L s⁻¹ (100 gal min⁻¹). There are two key differences between the treatment process assumed in the engineering evaluations

TABLE 3. Major Assumptions and Bases Used in Engineering Evaluations

assumption/basis	value	assumption/basis	value
Raw Material Costs		Cash Flow Analysis	
30% FeCl ₃	\$0.33/kg ^a	plant utility	90%
50% NaOH	\$0.33/kg ^a	escalation rate	2.5%/yr
emulsion polymer	\$3.30/kg ^a	years of operation	10 yr
filter aid	\$0.36/kg ^a	income tax rate	40%
filter cloth	\$1.00/m ²	creep investment	1.5%
filtered water	\$0.04/m ³	NPC ^b discount rates	12% and 25%
hazardous waste landfill disposal	\$0.19/kg wet sludge	depreciation (6-yr)	20%, 32%, 19%, 12%, 12%, 5%
electricity	\$0.045/kWh	Δ working capital	60 days cash costs
Other Cash Costs		Capital Investment Factors	
general plant overheads ^c	0.5% replacement inv. + 24% salaries, wages, & benefits	misc. equipment/ foundations, supports, platforms	5%/7%
maintenance	4% replacement inv.	field material, labor, insulation	17%
property taxes & insurance	0.75% replacement inv.	piping/instrument/ electrical	45%/16%/11%
operations (round-the-clock shift coverage)	\$430 000/yr	minor changes/ working conditions	2%/10%
technical exempt	\$160 000/yr	PG&S ^c /D&R ^d	10%
startup/project liaison	10%/2% new inv.	contingencies	25%
		MCC/ICR/ECR ^e	6%
		freight/QA/sales tax/procurement	11%
		engineering & home office/field indirects	20%/8%

^a 100% basis. ^b Net present cost. ^c Power, general, and service facilities. ^d Dismantlement and rearrangement. ^e Motor control center/instrument control center/electrical control center.

and that used in the experimental and modeling studies—use of FeCl₃ rather than Fe(NO₃)₂ and operation in a coprecipitation mode rather than a sorption mode. Investment, costs, and economics should not be used on an absolute basis to compare to other technology alternatives (such as ion exchange, alkaline precipitation, etc.); however, they can be safely used for a relative ranking of the multistage process alternatives.

The evaluations are based on the 10-step engineering evaluations methodology outlined in detail in ref 26. For each case, a process flow diagram was developed showing the necessary equipment pieces (pumps, tanks, clarifiers, filter presses, etc.) and process interconnections. From the process flow diagrams, facility scopes of work (i.e., a description of the physical facilities required to build the process) were developed, and operating requirements were defined (i.e., annual requirements for 50 wt % NaOH, 30 wt % FeCl₃, electricity, sludge disposal, etc.). On the basis of the facility scopes of work, capital investment was then estimated for each case using a factored, research guidance appraisal technique that is widely used within the chemical industry. Finally, armed with estimates for new capital investment and operating requirements, a 10-yr cash flow analysis was completed for each case to estimate annual cash operating cost and net present cost at both a 12% and 25% discount rate. Net present cost (NPC) was the economic measure of merit used to rank alternatives because it incorporates the effects of both new capital investment and ongoing cash operating costs over the life of the facility. A discount rate of 25% was chosen to rank the alternatives because it better reflects the opportunity cost of capital in situations where the supply of capital dollars is limited and other viable projects are competing for the same dollars (which is almost always the case in the chemical industry).

Table 3 summarizes the major assumptions used in the engineering evaluations. Bare equipment, raw material, utility, and waste disposal costs were obtained from various reliable sources (26–30). A process flow diagram for a two-stage, cross-flow, coprecipitation process is shown in Figure 2. A slightly to moderately anionic polyacrylamide emulsion polymer is added to the clarifier to improve solid–liquid separation. Process flow diagrams, facility scopes of work,

operating requirements, factored investment estimates, and 10-yr cash flow analyses are included in the Supporting Information.

Results and Discussion

Multistage Sorption Case Studies. Experimental data [Pb(II) effluent measured] and ESP modeling results [Pb(II) effluent model] for the multistage sorption case studies are summarized in Table 1. Experimental data are the arithmetic average of the effluent Pb(II) concentration measured in the three replicate studies for each stage of each case. Model data are ESP predictions based on the modified TLM and the parameters summarized in Table 2. To better assess the agreement between the measured and the model data, 95% confidence intervals (CI) were generated for each data point and are reported in Table 1. Details on the statistical tools, methodology, and uncertainty assumptions used to calculate the 95% CI are described in ref 31.

Briefly, confidence intervals for the measured values reflect the variation in or, more specifically, the *repeatability* of the three replicate studies for each stage of each case. Hence, the confidence intervals account for “within-the-same-batch” uncertainties in analytical/experimental procedures and equipment for the same operator conducting experiments with the same batch of ferrihydrite on the same day. These include analytical equipment, sample collection, sample handling, and sample processing errors as well as errors in pH calibration/control, reagent doses, etc. The Resampling Stats for Windows software (Resampling Stats, Inc., Arlington, Virginia) was used to estimate the 95% CI for the measured values. This software uses a bootstrap procedure (32, 33) to randomly generate *with replacement* *N* new samples of size, *n*, directly from the original sample. The number of new samples (*N*) is usually set at 10 000 or more, while the sample size (*n*), in this case, was 3. For this study, *N* was set equal to 10 000. The bootstrap procedure effectively creates a hypothetical “infinite” population that represents one’s best guess about the real population.

The 95% CI for the ESP model predictions, on the other hand, attempt to account for “between-batch” uncertainties in the model input parameters [i.e., pH, Pb(II) feed con-

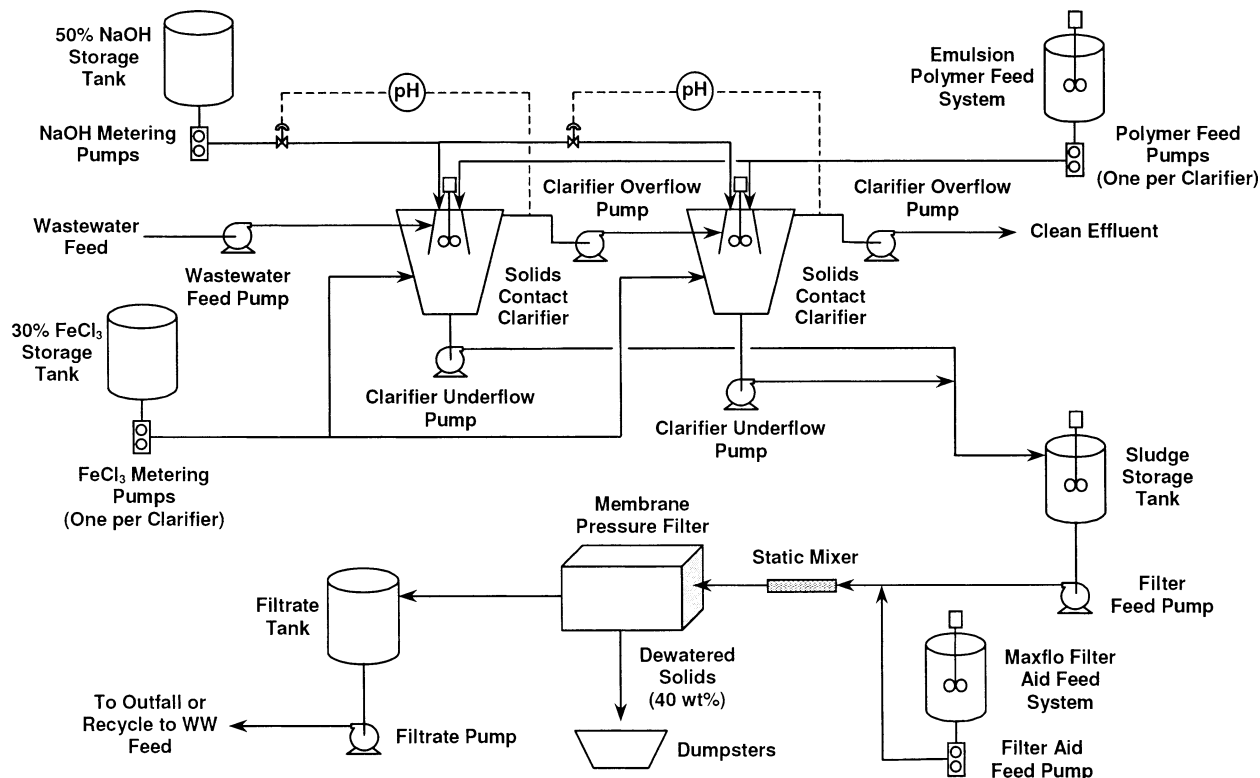


FIGURE 2. Process flow diagram for a two-stage cross-flow ferrihydrate coprecipitation process used in the engineering evaluations.

centration, ferrihydrate dose, NaNO_3 concentration, and mass of H_2O] as well as uncertainties in the regressed thermodynamic parameters (i.e., surface complexation equilibrium constants). Examples of between-batch uncertainties include differences in sorbent properties, reagent concentrations, and pH measurement equipment as compared to the original isotherm and edge studies used to determine the best-fit model parameters. Hence, the confidence intervals attempt to reflect the reproducibility of Pb(II)/ferrihydrate sorption studies on different days using different batches of ferrihydrate/reagents as well as the quality of the model fits of the acid–base titration and Pb(II) sorption data used to estimate the thermodynamic parameters in the first place. As described in ref 31, the OLI Software’s error analysis tool was first used to propagate input and thermodynamic parameter uncertainties through the multistage sorption model, yielding local extrapolation models that approximated the value of each output parameter of interest [i.e., effluent Pb(II) concentration and Pb(II) surface loading]. Monte Carlo simulations ($N = 10\,000$) of the OLI-generated local extrapolation models were then conducted with the Resampling Stats software to estimate the 95% CI for the model predictions.

In principle, the greater the overlap of the confidence intervals for the measured and model values, the higher the probability that the two values are the same. That is, one cannot say with confidence that the model and the measured values are statistically different. On the basis of the 95% confidence intervals reported in Table 1 (i.e., when model and experimental uncertainties are taken into account), the agreement between the model-predicted and measured effluent Pb(II) concentrations is very good. In all cases but three (stage 1 of case studies 1B and 3A and stage 4 of case study 3C), there is significant overlap of the 95% CI. More rigorous hypothesis testing using Resampling Stats indicated that the difference between the measured and the model values was statistically significant ($p < 0.05$) in only two cases (stage 1 of case studies 1B and 3A). On the basis of these results, the ESP model does an adequate job of predicting

the expected Pb(II) removal efficiency in a multistage operation.

Generalized Multistage Sensitivity Studies. Figure 3 shows the effects of influent Pb(II) concentration, pH, and number of equilibrium stages on the predicted effluent Pb(II) concentration from a multistage cross-flow adsorber operating with a total ferrihydrate dose of 1 g/L, equally split across the stages (i.e., 1 g/L in a one-stage system vs 0.5 g/L in each stage of a two-stage system). Figure 3a assumes perfect solid–liquid separations, while Figure 3b highlights the impact of 20 ppm suspended solids in the clarified effluent and 30 wt % solids in the settled iron sludge on effluent Pb(II) levels at pH 5.5. In both scenarios, the impact of pH and number of stages on Pb(II) removal is significant. For example, as shown in Figure 3a, a 10 ppm Pb(II)-containing water stream can be treated to only 80 ppb Pb(II) using a one-stage adsorber at pH 5.5; however, the addition of a second stage at the same pH will reduce the effluent Pb(II) concentration to approximately 2 ppb. On the other hand, adding a second stage and raising the pH to 6.5 will lower the effluent Pb(II) concentration another order of magnitude to approximately 0.2 ppb. The benefit realized by adding a second stage is most significant at low Pb(II) feed concentrations and at pH 5.5 and pH 6.5, where sorption of Pb(II) is highly favored. For pH 5.5 and pH 6.5, adding a second stage lowers the effluent Pb(II) concentration by 30–100-fold. The minimal impact of a second stage at pH 4.5 is the result of operating along the lower portion of the pH sorption edge for Pb(II).

The impact of solids carryover in the clarified effluent is to reduce Pb(II) removal efficiency. As shown in Figure 3b, predicted effluent Pb(II) concentrations at pH 5.5 increase by 2–50-fold when compared to the model predictions based on perfect solid–liquid separations. As might be expected, the benefit gained by adding a second equilibrium stage is diminished as solids carryover increases. Consider the same 10 ppm Pb(II)-containing water stream discussed above for Figure 3a. On the basis of Figure 3b, the predicted effluent

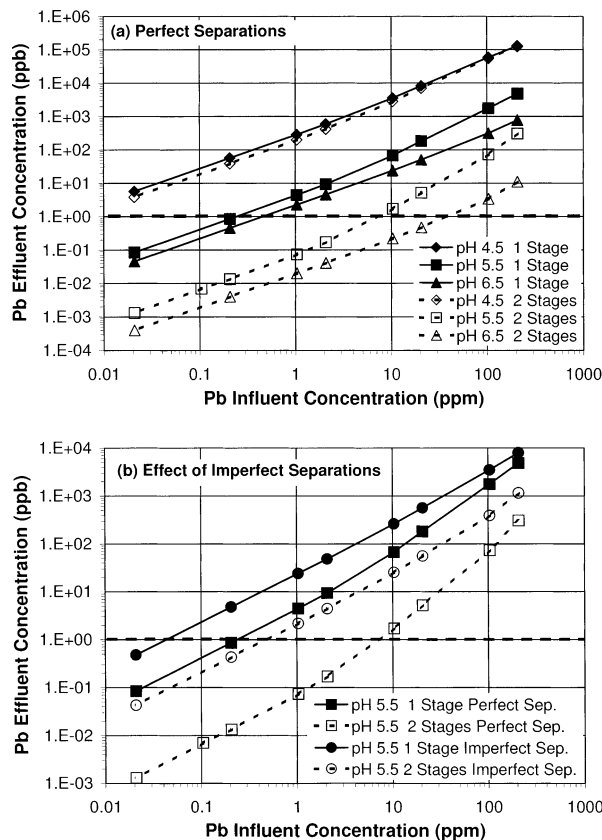


FIGURE 3. Impact of influent Pb(II) concentration, pH, and number of equilibrium stages on the effluent Pb(II) concentration in one- and two-stage cross-flow adsorbers operating with a fixed total ferrihydrite dose of 1 g/L (1 g/L equally split between stages in two-stage system). In panel a, perfect solid–liquid separations are assumed. In panel b, the impact of imperfect solid–liquid separations (20 ppm suspended solids in clarified effluent and 30 wt % solids in the settled sludge) on Pb(II) removal at pH 5.5 is shown. Model predictions are based on the modified triple-layer model using a 0.01 M NaNO₃ background electrolyte solution and parameters summarized in Table 2.

Pb(II) concentration for a two-stage adsorber operating at pH 5.5 is about 30 ppb (instead of 2 ppb) when more realistic solid–liquid separation efficiencies are assumed (20 ppm suspended solids in the clarified effluent and 30 wt % solids in the settled iron sludge).

Similarly, Figure 4a,b displays the impacts of influent Pb(II) concentration, pH, and number of equilibrium stages on the total required ferrihydrite dose in multistage cross-flow Pb(II) adsorbers operating with a fixed effluent Pb(II) concentration of 1 ppb. Figure 4a assumes perfect solid–liquid separations; Figure 4b highlights the impact of 20 ppm suspended solids in the clarified effluent and 30 wt % solids in the settled iron sludge on effluent Pb(II) concentration at pH 5.5. As in Figure 3, the impact of pH and number of stages on Pb(II) removal efficiency is significant. For example, as shown in Figure 4a, total ferrihydrite consumption for the same hypothetical 10 ppm Pb(II)-containing water stream can be reduced from ~40 g/L using a one-stage adsorber at pH 5.5 to ~1.2 g/L using a two-stage adsorber at pH 5.5 to ~0.45 g/L using a two-stage adsorber at pH 6.5. In this case, the beneficial impact of adding a second stage is most significant at higher Pb(II) feed concentrations and pH.

The negative impact of solids carryover in the clarified effluent is also displayed in Figure 4b. Predicted total ferrihydrite doses at pH 5.5 increase by 4–7-fold when compared to the predicted doses assuming perfect solid–liquid separations. For the same 10 ppm Pb(II)-containing

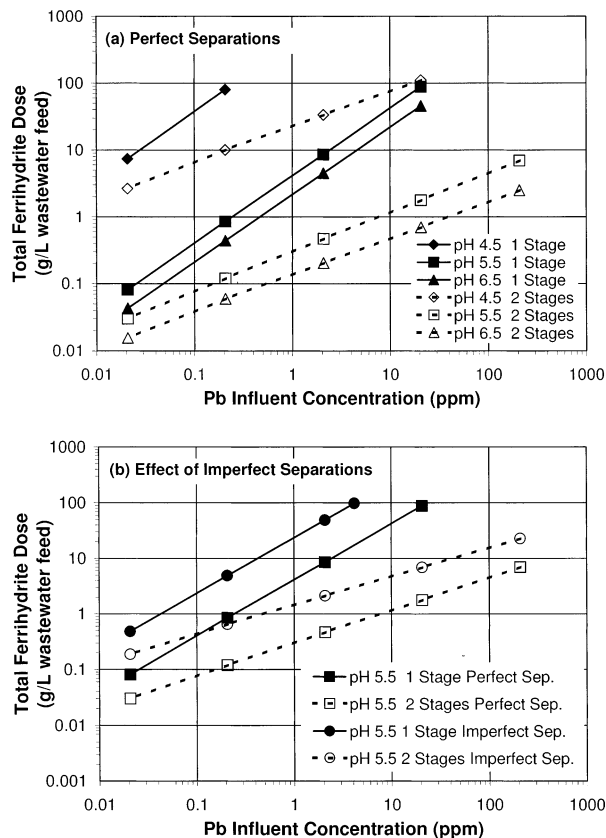


FIGURE 4. Impact of influent Pb(II) concentration, pH, and number of equilibrium stages on total ferrihydrite consumption in one- and two-stage cross-flow adsorbers operating with a fixed effluent Pb(II) concentration of 1 ppb. Ferrihydrite is equally split between stages in the two-stage system. In panel a, perfect solid–liquid separations are assumed. In panel b, the impact of imperfect solid–liquid separations (20 ppm suspended solids in clarified effluent and 30 wt % solids in the settled sludge) on ferrihydrite consumption at pH 5.5 is shown. Model predictions are based on the modified triple-layer model using a 0.01 M NaNO₃ background electrolyte solution and parameters summarized in Table 2.

water stream discussed above for Figure 4a, the required total ferrihydrite dose for a two-stage adsorber operating at pH 5.5 is about 5 g/L (instead of 1.2 g/L) when more realistic solid–liquid separation efficiencies are assumed.

Finally, Figure 5 shows the impact of number of equilibrium stages on total ferrihydrite dose as a function of Pb(II) feed concentration for both cross-flow (Figure 1a) and true countercurrent-flow (Figure 1b) arrangements. Figure 5 assumes operation at pH 5.5, 10 ppb Pb(II) total in the clarified effluent, 20 ppm suspended solids carryover, and 30 wt % solids in the iron sludge. It is apparent from Figure 5 that the benefits of staging diminish as the number of equilibrium stages increases. By three to four stages, the dose curves begin to level out. Figure 5 also highlights the ferrihydrite consumption penalty realized by operating in a cross-flow arrangement instead of a true countercurrent-flow arrangement. Total ferrihydrite doses are 2–4 times higher for the cross-flow arrangement for two or more equilibrium stages.

Economic Benefits of Staging. Table 4 presents the results of engineering evaluations for the multistage sorption case studies summarized in Table 1, assuming a volumetric wastewater flow rate of 6.3 L s⁻¹. A key principle of engineering evaluations is that process flow sheets and scopes of work should be based on equivalent outcomes [i.e., the same effluent Pb(II) concentration] in order to fairly compare alternatives. Case studies 2A–2C adhere to this principle

TABLE 4. Engineering Evaluation Results for Multistage Sorption Case Studies at 6.3 L s⁻¹ Volumetric Flow Rate

case	no. of stages	g of fh ^a /L in each stage ^b	Pb(II) feed concn (ppm)	2002 investment (\$1000)	2004 cash operating cost (\$1000/yr)	2002 NPC ^c at 12% (\$1000)	2002 NPC ^c at 25% (\$1000)
1A	1	1.0	103.6	2 400	710	4 900	3 200
1B	2	0.5	103.6	2 800	770	5 500	3 600
2A	1	4.65	10.36	4 100	2,180	12 600	7 400
2B	2	0.253	10.36	2 500	540	4 300	2 900
2C	3	0.08	10.36	2 800	500	4 400	3 000
3A	1	0.4	103.6	2 000	450	3 500	2 400
3B	2	0.2	103.6	2 500	520	4 200	2 900
3C	4	0.1	103.6	3 400	640	5 400	3 800

^a Ferrihydrite. ^b Total ferrihydrite consumption equals the ferrihydrite dose in each stage times the number of stages (e.g., for case 3C, total ferrihydrite consumption is 0.1 g/L × 4 stages = 0.4 g/L total. ^c Net present cost.

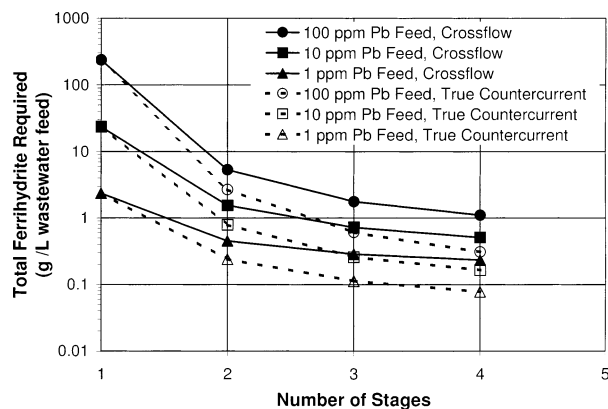


FIGURE 5. Impact of the number of equilibrium stages and influent Pb(II) concentration on total ferrihydrite consumption in cross-flow and true countercurrent-flow adsorbers operating at pH 5.5 with a fixed effluent Pb(II) concentration of 10 ppb, 20 ppm suspended solids in clarified effluent, and 30 wt % solids in the settled sludge. Ferrihydrite is equally split between stages in the multistage systems. Model predictions are based on the modified triple-layer model using a 0.01 M NaNO₃ background electrolyte solution and parameters summarized in Table 2.

having been designed to achieve an effluent Pb(II) concentration of ~10 ppb from the final stage. For this reason, NPC_{25%} values for each of these cases can be compared to choose the most cost-effective alternative(s). In other words, they can provide insight on the economic benefit of additional equilibrium stages. Case studies 1 and 3, on the other hand, are not based on equivalent outcomes [i.e., the effluent Pb(II) concentration varies between alternatives]. However, they do provide valuable insights on the incremental investment and net present cost associated with adding equilibrium stages to lower the effluent Pb(II) concentration at a fixed total ferrihydrite dose.

The results for case studies 2A–2C in Table 4 clearly show that the addition of a second equilibrium stage makes economic sense (NPC_{25%} of \$2 900 000 for two stages vs \$7 400 000 for one stage). The additional investment and ongoing operating costs associated with handling, dewatering, and disposing of an order of magnitude more iron sludge are substantial [4.65 g/L total for case 2A vs 0.506 g/L total (0.253 g/L per stage × 2 stages) for case 2B]. On the other hand, the addition of a third stage just about breaks even (NPC_{25%} of \$3 000 000 for 3 stages vs \$2 900 000 for 2 stages); therefore, the additional operational complexity associated with three stages versus two is probably not justified. In this case, the reduction in sludge from case 2B to case 2C is only about 2-fold [0.506 g/L total for case 2B vs 0.24 g/L total (0.08 g/L per stage × 3 stages) for case 2C]. The use of four or more stages would almost certainly result in an NPC_{25%} > \$3 000 000.

The results for case studies 1 and 3 indicate that the incremental investment and NPC_{25%} for moving to a multistage operation are both on the order of \$400 000–500 000 per added stage. This compares to one-stage (i.e., base case) NPC_{25%} values of \$3 200 000 and \$2 400 000 for case studies 1A and 3A, respectively. In other words, the incremental NPC_{25%} for an additional stage is approximately 15–20% of the base-case NPC_{25%}. For case study 1, a second stage at the same total ferrihydrite dose results in more than an order of magnitude reduction in effluent Pb(II) concentration. For case study 3, each incremental stage provides about an order of magnitude reduction in effluent Pb(II) concentration on the basis of the experimental data reported in Table 1.

In summary, chemical equilibrium modeling is an important engineering tool because it enables one to predict the removal of contaminants, such as Pb(II), from aqueous streams under different environmental conditions and at different sorbent concentrations. More importantly, the modeling approach used in this research is consistent with the macroscopic and spectroscopic findings for these systems that have been discussed in detail in ref 18. Such a modeling approach can significantly improve current approaches to risk assessment and waste management. As regulated trace metal concentrations in water discharges are pushed to ppb and lower levels, multistage contacting schemes will likely provide substantial economic benefits when sorption onto or coprecipitation with amorphous materials, such as ferrihydrite, are being considered. Table 4 shows that a 2–3-stage sorption process can provide significant economic savings when compared to a 1-stage process operating with the same target effluent Pb(II) concentration. In addition, this research has shown that a steady-state process flow sheet simulator, such as OLI Systems' ESP software, can adequately predict Pb(II) removal in a multistage ferrihydrite adsorber using the triple-layer surface complexation model calibrated with macroscopic and spectroscopic Pb(II) sorption data. Finally, the collective body of work presented in refs 18, 19, 31, and this paper helps to show how fundamental macroscopic and spectroscopic metal sorption data, coupled with surface complexation modeling, can be practically used to help solve industrial trace metal emissions problems.

Acknowledgments

This research was supported by funding from the DuPont Company and the State of Delaware through the Delaware Research Partnership. The authors particularly thank Drs. Jehangir Vevai and Hugh Campbell (DuPont Company) and Dr. Marshall Rafal (OLI Systems, Inc.) for their financial support. Important contributions to the engineering evaluations were provided by Stephen W. Constable and Dr. Ernest Mayer from DuPont. We are also very grateful to three anonymous reviewers for their comments.

Supporting Information Available

Graph showing an ESP block flow diagram; two figures showing process flow diagrams for one- and two-stage treatment processes; detailed results for the engineering evaluations of the multistage sorption case studies in Table 1. This material is available free of charge via the Internet at <http://pubs.acs.org>.

Nomenclature

A_s	specific surface area of sorbent (m^2/g)
C_1	inner-layer capacitance term for triple-layer model (faraday/ m^2)
C_2	outer-layer capacitance term for triple-layer model (faraday/ m^2)
K_j^{int}	intrinsic or thermodynamic equilibrium constant
K_{a1}^{int}	intrinsic acidity constant for the surface deprotonation reaction: $\equiv\text{FeOH}_2^+ = \equiv\text{FeOH} + \text{H}^+$
K_{a2}^{int}	intrinsic acidity constant for the surface deprotonation reaction: $\equiv\text{FeOH} = \equiv\text{FeO}^- + \text{H}^+$
N	number of resamples
n	sample size
N_s	surface site density (mol of sites/mol of sorbent)
$\gamma_{\text{Pb}^{2+}}$	activity coefficient for the Pb^{2+} ion in the bulk solution
γ_s	lumped surface activity coefficient used in OLI model to account for nonidealities of the surface complex species per ref 19

Literature Cited

- Gurian, P. L.; Small, M. J.; Lockwood, J. R.; Schervish, M. J. *Environ. Sci. Technol.* **2001**, *35*, 4414–4420.
- U.S. EPA. *Fed. Regist.* **2001**, *66* (14), 6976–7066.
- U.S. EPA. *Fed. Regist.* **2001**, *66* (202), 53044–53048.
- U.S. EPA. *Fed. Regist.* **2000**, *65* (135), 43586–43670.
- Wenning, R. J. *Contam. Soil Sediment Water* **2001**, June/July, 49–54.
- Dyer, J. A.; Scrivner, N. C.; Dentel, S. K. *Environ. Prog.* **1998**, *17* (1), 1–7.
- Merrill, D. T.; Maroney, P. M.; Parker, D. S. *Trace Element Removal by Coprecipitation with Amorphous Iron Oxyhydroxide: Engineering Evaluation*; CS-4087; Electric Power Research Institute: Palo Alto, CA, 1985.
- Schultz, M. F.; Benjamin, M. M.; Ferguson, J. F. *Environ. Sci. Technol.* **1987**, *21*, 863–869.
- Edwards, M.; Benjamin, M. M. *J. Water Pollut. Control Fed.* **1989**, *61*, 481–490.
- Theis, T. L.; Iyer, R.; Ellis, S. K. *J. Am. Water Works Assoc.* **1992**, *84*, 101–105.
- Fan, H.; Anderson, P. R. In *Proceedings of the 50th Industrial Waste Conference*, May 8–10, 1995; Wukasch, R. F., Dalton, C. S., Eds.; Lewis Publishers: Boca Raton, FL, 1996; pp 217–226.
- Gao, Y.; Sengupta, A. K.; Simpson, D. *Water Res.* **1995**, *29*, 2195–2205.
- Smith, E. H. *J. Environ. Eng.* **1998**, *124*, 913–920.
- Smith, E. H.; Amini, A. *J. Environ. Eng.* **2000**, *126*, 58–65.
- Reyes-Labarta, J. A.; Grossmann, I. E. *AIChE J.* **2001**, *47*, 2243–2252.
- Van Vliet, R. E.; Tiemersma, T. P.; Krooshof, G. J.; Iedema, P. D. *Ind. Eng. Chem. Res.* **2001**, *40*, 4586–4595.
- Zomosa, A. *Miner. Metall. Process.* **1990**, *7*, 118–120.
- Trivedi, P.; Dyer, J. A.; Sparks, D. L. *Environ. Sci. Technol.* **2003**, *37*, 908–914.
- Dyer, J. A.; Trivedi, P.; Scrivner, N. C.; Sparks, D. L. *Environ. Sci. Technol.* **2003**, *37*, 915–922.
- Davis, J. A.; James, R. O.; Leckie, J. O. *J. Colloid Interface Sci.* **1978**, *63*, 480–499.
- Davis, J. A.; Leckie, J. O. *J. Colloid Interface Sci.* **1978**, *67*, 90–107.
- Hayes, K. F.; Leckie, J. O. In *Geochemical Processes at Mineral Surfaces*; Davis, J. A., Hayes, K. F., Eds.; ACS Symposium Series 323; American Chemical Society: Washington, DC, 1986; pp 114–141.
- Hayes, K. F.; Leckie, J. O. *J. Colloid Interface Sci.* **1987**, *115*, 564–572.
- Sverjensky, D. A.; Sahai, N. *Geochim. Cosmochim. Acta* **1996**, *60*, 3773–3797.
- Hayes, K. F.; Katz, L. E. In *Physics and Chemistry of Mineral Surfaces*; Brady, P. V., Ed.; CRC Press: Boca Raton, FL, 1996; pp 147–223.
- Mulholland, K. L.; Dyer, J. A. *Pollution Prevention: Methodology, Technologies and Practices*; American Institute of Chemical Engineers: New York, 1999.
- Schnell Publishing. *Chem. Market Rep.* **2002**, *261* (12), 16–19.
- Gumerman, R. C.; Burris, B. E.; Hansen, S. P. *Small Water System Treatment Costs*; Noyes Data Corporation: Park Ridge, NJ, 1986.
- DuPont Investment Technologies. *RGA Software, Version 3.1*; DuPont Company: Wilmington, DE, 1998.
- DuPont Sourcing. Personal communications.
- Dyer, J. A. *Advanced Approaches for Modeling Trace Metal Sorption in Aqueous Systems*. Ph.D. Dissertation, University of Delaware, Newark, DE, 2002.
- Diaconis, P.; Efron, B. *Sci. Am.* **1983**, *248* (5), 116–130.
- Simon, J. L. *Resampling: The New Statistics*; Resampling Stats, Inc.: Arlington, VA, 1997.

Received for review June 7, 2002. Revised manuscript received December 6, 2002. Accepted December 13, 2002.

ES025855L